The complementary contribution of each order topology into the synchronization of multi-order networks

Xiaomin Ren,[1] Youming Lei,[1] Celso Grebogi,[2] and Murilo S. Baptista[2]
[1)]*School of Mathematics and Statistics, Northwestern Polytechnical University, Xi'an 710072, China*
[2)]*Institute for Complex Systems and Mathematical Biology, University of Aberdeen, Aberdeen, AB24 3UE, UK*

(*Electronic mail: murilo.baptista@abdn.ac.uk)

(*Electronic mail: leiyouming@nwpu.edu.cn)

(Dated: 2 November 2023)

Higher-order interactions improve our capability to model real-world complex systems ranging from physics and neuroscience to economics and social sciences. There is great interest nowadays in understanding the contribution of higher-order terms to the collective behavior of the network. In this work, we investigate the stability of complete synchronization of complex networks with higher-order structures. We demonstrate that the synchronization level of a network composed of nodes interacting simultaneously via multiple orders is maintained regardless of the intensity of coupling strength across different orders. We articulate that lower-order and higher-order topologies work together complementarily to provide the optimal stable configuration, challenging previous conclusions that higher-order interactions promote the stability of synchronization. Furthermore, we find that simply adding higher-order interactions based on existing connections, as in simple complexes, does not have a significant impact on synchronization. The universal applicability of our work lies in the comprehensive analysis of different network topologies, including hypergraphs and simplicial complexes, and the utilization of appropriate rescaling to assess the impact of higher-order interactions on synchronization stability.

Networks with higher-order interactions have emerged as a significant component in modeling real-world complex systems. They describe systems whose variables interact with multiple variables simultaneously, forming complex structures beyond those found in networks whose nodes interact in a pairwise manner. Exploring the contribution of higher- order interactions to the synchronization of networks is of major interest. Previous works have claimed that the introduction of higher-order interactions to networks whose nodes are connected by either pairwise interactions or lower-order interactions can promote synchronization based on the network topology. In this work, we demonstrate that this assertion does not hold. We first show that the inclusion of higher-order interactions to a network with a lower-order structure does indeed lead to synchronization enhancement, but only if the higher-order interactions are included without an unbiased rescaling in the coupling strengths of the connections. By using our derived unbiased rescaling, which incorporates information about the topologies of the connections and does not favor one order structure in detriment of another, we show that the inclusion of higher-order interactions does not alter the state of synchronization. In fact, there is an optimal value of the coupling strength for which the state of synchronization is maximal by the inclusion of higher-order structures to networks formed by lower-order structures. It is the lower-order and higher-order topologies working together complementarily that provide the optimal stable configuration. This demonstrates that the focus of research in this topic should shift from seeking to achieve enhancement or inhibition of synchronization by including higher-order structures, to the goal of seeking to find configurations where both the lower-order and the higher-order interactions mutually contribute to the increase of synchronization.

I. INTRODUCTION

Networks are widely utilized to model coupled dynamical processes in science and technology[1,2]. Traditionally, these models have focused on pairwise interactions between dynamical units, represented by the edges or links of a graph[3]. However, higher-order interactions, involving simultaneous interactions among groups of units, have been shown to be ubiquitous. Examples of such higher-order interactions can be found in the brain[4,5], ecological communities[6,7], and collaboration networks[8,9]. Recently, there has been significant research aimed at understanding how the interplay between higher-order structures and dynamical processes governs collective behaviors[10,11]. To effectively capture connections of different orders, some network structures, such as hypergraphs[12–14] and simplicial complexes[15,16] have been introduced to represent the higher-order networks.

Synchronization[17,18] is a collective behavior that strongly relies on the underlying interaction structure. It has many crucial applications in various systems. A handful of studies have observed synchronization in neuronal networks[19–22], sensor networks[23], multilayer networks[24–27], and time-varying networks[28]. Recent works showed that higher-order interactions have notable effects on synchronization. For instance, they can promote explosive synchronization[29–32], multistability[33,34], cluster synchronization[31], chimera[35–37],

etc. For the stability of synchronization, the Master Stability Function has been applied to the stability analysis of several special cases of higher-order networks[38,39]. Along with these studies, mathematical approaches, such as the mean-field approximation[14,29,35] and the Laplacian description[39,40] have been extended to incorporate higher-order structures.

One of the most prominent and extensively studied network models for analyzing the stability of synchronization in complex networks is the Kuramoto network model[41–44], which has also been generalized to higher order. Through linearization, the stability of the complete synchronous mode in the higher-order Kuramoto network is associated with the properties of the generalized Laplacian[40,45]. Beyond the Kuramoto network, a general framework was proposed in Ref.[39] to study the stability of synchronization in a generic system with arbitrary interaction orders and coupling functions. Following it, similar stability analyses were proposed to study the emergency of complete synchronization in directed hypergraphs[46] and networks with multiple interaction layers[47].

Previous works[45,48,49] have considered using a higher-order proportion $\alpha, \alpha \in [0,1]$ to address the influence of specific order interactions on the collective behavior of higher-order networks. Considering a multi-order network formed by 2-order structures (one pairwise order-1 and the other higher-order), they first normalized the coupling strength among nodes belonging to a specific order structure by dividing it by the average degree of connection in that structure. Then, they multiplied the coupling strength of higher-order interactions by α, and that of the lower-order interactions by $(1-\alpha)$. By employing this strategy, networks were constructed with a combination of order-1 and higher-order terms, ensuring that the overall coupling strength among units remains consistent as higher-order structures are incorporated into the model. By examining how the synchronization changes with α, those studies drew conclusions regarding the role of higher-order interactions. For example, the work in Ref.[45] suggested that synchronization is promoted by the higher-order structure, if they are hypergraphs, but not promoted if they are simplicial complexes.

As the stability of multi-order networks is a function that does not only depend on the coupling strength and the average degree, but rather on the whole network structure[50,51] and the coupling functions[39], the normalization (dividing by the average degree) and parametrization (multiplying by α) used in Refs.[40,45] is prone to oversight the role of higher-order interactions in shaping the collective behavior of the whole network. Therefore, claims about whether higher-order interactions can or not promote synchronization should be taken with caution.

In this work, we introduce a further parametrization to the network, a rescaling factor R. This rescaling factor is derived from the eigenmode of the variational equations and takes into account the coupling strength, structure of the network, and coupling function. We demonstrate that it is always possible to find a constant rescaling that can make a network with arbitrary interaction order exhibit an equivalent stability of synchronization compared to another network with any other interaction order. Specifically, we provide examples using Kuramoto networks as a prototype to assert that there is always a low-order pairwise network that can achieve the same level of stability as a higher-order network.

To study the impact of higher-order interactions more fairly, we introduce this rescaling factor to a network with two interaction orders. Subsequently, we employ the Maximum Transverse Lyapunov Exponent (MTLE) to examine the synchronization stability within this rescaled network. In contrast to the findings in Ref.[45], we articulate that the addition of higher-order structures neither promotes nor inhibits synchronization. The synchronization scenario is actually even more diverse. The stability (measured by the MTLE) is maximal at an optimal value of α. It is not whether higher order that improves (or not) synchronization, but simply that these two topologies work together complementarily to provide the optimal stable configuration. If the higher-order structure is a simplicial complex, the underlying topology remains the same as the interaction order increases. The higher-order proportion α does not have significant influence on the synchronization so that the MTLEs remain roughly invariant with α. Especially, when the Laplacians commute, we demonstrate that the MTLE is a constant function with α. Furthermore, if the network grows in size, regardless of the type of the higher-order structure, the MTLEs remain roughly invariant. Thus, the stability of the multi-order network does not typically depend on higher-order interactions proportion α.

II. RESULTS

A. The rescaling between networks with interactions of different orders

We consider a coupled dynamical system with order d interactions. Its evolution is governed by

$$\dot{\mathbf{x}}_i = \mathbf{f}(\mathbf{x}_i) + \sigma_d \sum_{j_1=1}^{N} \cdots \sum_{j_d=1}^{N} a^{(d)}_{ij_1\ldots j_d} \mathbf{g}^{(d)}\left(\mathbf{x}_i, \mathbf{x}_{j_1}, \ldots, \mathbf{x}_{j_d}\right), \quad (1)$$

where $\mathbf{x}_i \in \mathbb{R}^m$ is the vector state of node i, with $i = 1, \ldots, N$. The uncoupled dynamics of each node is identical, which is $\dot{\mathbf{x}}_i = \mathbf{f}(\mathbf{x}_i).\sigma_d$ is the coupling strength of the $(d+1)-$ body interactions. $\mathbf{g}^{(d)} : \mathbb{R}^{(d+1)\times m} \to \mathbb{R}^m$ is the coupling function of order d, which satisfies the synchronization noninvasive condition $\mathbf{g}^{(d)}(\mathbf{x}, \mathbf{x}, \ldots, \mathbf{x}) = 0$. The interaction architecture of order d is encoded in the adjacency tensor $\left(a^{(d)}_{ij_1\ldots j_d}\right)$, where $a^{(d)}_{ij_1\ldots j_d} = 1$, if nodes $(i, j_1, \ldots, j_d)$ belong to an order d interaction simultaneously, and $a^{(d)}_{ij_1\ldots j_d} = 0$, otherwise.

To analyze the stability of the synchronization, we introduce a small perturbation $\delta\mathbf{x}_i = \mathbf{x}_i - \mathbf{x}^s$ around the synchronization manifold $\mathbf{x}^s(t) = \mathbf{x}_1(t) = \ldots = \mathbf{x}_N(t)$. Applying the linear stability analysis to higher-order networks (Ref.[39]), we obtain the variational equations given by

$$\delta\dot{\mathbf{x}}_i = J\mathbf{f}(\mathbf{x}^s)\,\delta\mathbf{x}_i - \sigma_d \sum_{j=1}^{N} L^{(d)}_{ij} J G^{(d)} \delta\mathbf{x}_j, \quad (2)$$

where $L^{(d)}$ is the generalized Laplacian of order d, a higher-order extension of the classical Laplacian of the

graph (see Appendix B for its definition). J is the Jacobian operator. The Jacobian matrices for function $\mathbf{f}$ and coupling function $\mathbf{g}^{(d)}\left(\mathbf{x}_i,\mathbf{x}_{j_1},\ldots,\mathbf{x}_{j_d}\right)$ are represented by $J\mathbf{f}(\mathbf{x}^s)$ and $JG^{(d)} = J_1\mathbf{g}^{(d)}(\mathbf{x}^s,\ldots,\mathbf{x}^s) + J_2\mathbf{g}^{(d)}(\mathbf{x}^s,\ldots,\mathbf{x}^s) + \ldots + J_d\mathbf{g}^{(d)}(\mathbf{x}^s,\ldots,\mathbf{x}^s)$, in which $J_k\mathbf{g}^{(d)}(\mathbf{x}^s,\ldots,\mathbf{x}^s)$ is $\partial g^{(d)}\left(\mathbf{x}_i,\ldots,\mathbf{x}_{j_d}\right)/\partial\mathbf{x}_{j_k}\big|_{(\mathbf{x}^s,\ldots,\mathbf{x}^s)}$.

By combining all N variational equations with the Kronecker product, we derive the equation for the perturbation $\delta\mathbf{x} = \left[\delta\mathbf{x}_1^T,\delta\mathbf{x}_2^T,\ldots,\delta\mathbf{x}_N^T\right]^T$, which is

$$\delta\dot{\mathbf{x}} = \left[I_N\otimes J\mathbf{f}(\mathbf{x}^s) - \sigma_d L^{(d)}\otimes JG^{(d)}\right]\delta\mathbf{x}. \tag{3}$$

Following the steps to derive the Master Stability Equation in Refs.[52,53], Eq. (3) can be decoupled into N independent eigenmodes by diagonalizing the generalized Laplacian $L^{(d)}$, that is $V^{-1}L^{(d)}V = \mathrm{diag}(\lambda_1,\lambda_2,\ldots,\lambda_N)$, where $0=\lambda_1<\lambda_2\leq\ldots\leq\lambda_N$ are eigenvalues and $V=[v_1,v_2,\ldots,v_N]$ is the matrix of the eigenvectors. By the transformation $\xi = \left(V^{-1}\otimes I_m\right)\delta\mathbf{x}$, we obtain the dynamics for each eigenmode

$$\dot{\xi}_i = \left[J\mathbf{f}(\mathbf{x}^s) - \boldsymbol{\lambda}_i\left(\sigma_d L^{(d)}\right)JG^{(d)}\right]\xi_i, \tag{4}$$

where $\boldsymbol{\lambda}_i:\mathbb{R}^{(N\times N)}\to\mathbb{R}$ is a function calculating the i-th eigenvalue of a matrix. Among all the N eigenmodes, the second eigenmode ξ_2 corresponding to the smallest non-zero eigenvalue of the Laplacian is the dominant mode. For the case of the unbounded synchronization region (synchronization will not be lost as the coupling strength increases), if the second eigenmode is stable, all the other eigenmodes are stable. The identical second eigenmode indicates equivalent stability of synchronization. From Eq. (4), assuming that all the systems with different orders have the same $J\mathbf{f}(\mathbf{x}^s)$, the stability of synchronization is determined by the coupling strength (σ_d), the coupling structure $(\boldsymbol{\lambda}_i)$, and the Jacobian of coupling function $(JG^{(d)})$.

Based on the above analysis, the synchronization stability of two systems with interaction orders d_1 and d_2 are equivalent, if their second eigenmodes are the same. We suppose the Jacobian $J\mathbf{f}(\mathbf{x}^s)$ is identical for systems with any order. To achieve this equivalence, we introduce a rescaling R, which satisfies $R\boldsymbol{\lambda}_2\left(\sigma_{d_1}L^{(d_l)}\right)JG^{(d_1)} = \boldsymbol{\lambda}_2\left(\sigma_{d_2}L^{(d_2)}\right)JG^{(d_2)}$. Then the definition of a rescaling comes as

$$R = \frac{\boldsymbol{\lambda}_2\left(\sigma_{d_2}L^{(d_2)}\right)JG^{(d_2)}}{\boldsymbol{\lambda}_2\left(\sigma_{d_1}L^{(d_1)}\right)JG^{(d_1)}}. \tag{5}$$

To achieve a constant rescaling R, which does not depend on system states, the Jacobian matrices $JG^{(d_1)}$ and $JG^{(d_2)}$ should be the same (e.g., the natural coupling[39]) or be constants (e.g., $\sin\left(\sum_{k=1}^{d}\theta_{j_k} - d\theta_i\right)$ or the linear coupling functions).

B. The equivalent synchronization stability of rescaled Kuramoto network and higher-order Kuramoto network

In this section, we focus on the rescaling of an order-1 Kuramoto network, which consists of only pairwise interactions, and demonstrate its dynamics approaching the synchronization manifold, which is equivalent to that of an order-2 Kuramoto network with three-body interactions only. By "equivalent," we refer to the similarity in the evolution of the order parameter and the proximity of unit trajectories to the synchronization manifold in both networks. Notably, after rescaling, Eq. (4), the second eigenmodes of both networks are identical. All the simulations in this work are conducted both on hypergraphs and simplicial complexes (see Appendix A for their definitions, and how to construct them).

It should be noted that the purpose of this section is to construct two networks with different orders but the same synchronization stability. In the next section, we will build a multi-order network based on these two networks. Although we prove that higher-order and lower-order networks can have the same synchronization stability, this is not the main reason for us to draw the conclusion that high-order interactions neither promote nor inhibit the stability of synchronization.

The order-1 Kuramoto network is described by

$$\dot{\theta}_i = \omega + \sigma_1\sum_{j_1=1}^{N}a_{ij_1}^{(1)}\sin\left(\theta_{j_1}-\theta_i\right), \tag{6}$$

where θ_i is the phase of node i, ω is the natural frequency, and $a_{ij_1}^{(1)}$ is the element of the adjacency matrix that encodes the network topology.

The order-2 Kuramoto network is described by

$$\dot{\theta}_i = \omega + \sigma_2\sum_{j_1=1}^{N}\sum_{j_2=1}^{N}a_{ij_1j_2}^{(2)}\sin\left(\theta_{j_1}+\theta_{j_2}-2\theta_i\right), \tag{7}$$

where $a_{ij_1j_2}^{(2)}$ is the element of the order-2 adjacency tensor. If $a_{ij_1j_2}^{(2)}=1$, there exists a 3-body interaction involving nodes (i,j_1,j_2), otherwise, $a_{ij_1j_2}^{(2)}=0$.

Since in the Kuramoto network, the Jacobian $JG^{(d)}=d$ is a constant (see Appendix C for details). According to Eq. (5), the rescaling of the order-1 Kuramoto network is

$$R = \frac{\boldsymbol{\lambda}_2\left(\sigma_2L^{(2)}\right)JG^{(2)}}{\boldsymbol{\lambda}_2\left(\sigma_1L^{(1)}\right)JG^{(1)}} = \frac{2\sigma_2\boldsymbol{\lambda}_2\left(L^{(2)}\right)}{\sigma_1\boldsymbol{\lambda}_2\left(L^{(1)}\right)}. \tag{8}$$

And the rescaled order-1 Kuramoto network is given by

$$\dot{\theta}_i = \omega + R\sigma_1\sum_{j_1=1}^{N}a_{ij_1}^{(1)}\sin\left(\theta_{j_1}-\theta_i\right). \tag{9}$$

We proceed to demonstrate the equivalence of synchronization between the rescaled order-1 Kuramoto network in Eq. (9) and the order-2 Kuramoto network in Eq. (7). When two dynamical systems exhibit the same linear stability of the complete synchronous manifold, trajectories close to the synchronization manifold approach the synchronization manifold similarly. Assuming that the network is sufficiently stable, trajectories should take a similar time to approach the manifold. But, in the case of the systems studied here, linear stability implies Lyapunov stability, and thus, similar stability results

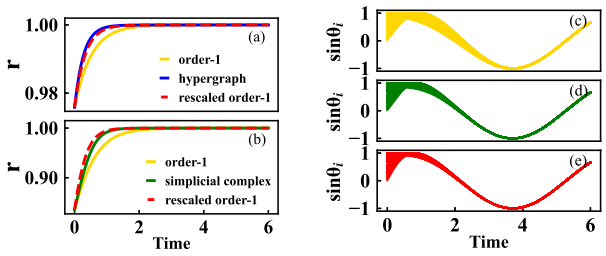

FIG. 1. (a) depicts the order parameters over time for the order-1 Kuramoto network (yellow), order-2 Kuramoto network (blue), and rescaled order-1 Kuramoto network (red). In (a), all the networks are represented by hypergraphs. In (b), those three Kuramoto networks are represented by simplicial complexes. (c)-(e) correspond to the phase evolution of the Kuramoto networks in (b). Here, the parameters are natural frequency $\omega = 1$, coupling strength $\sigma_1 = 1/ < k^{(1)} >, \sigma_2 = 1/\left(2 < k^{(2)} >\right), < k^{(d)} >$ is the averaged degree, the number of nodes $N = 100$, edge probability for d-hyperedge $p_1 = 0.8, p_2 = 0.01$, and edge probability for the simplicial complex $p = 0.5$. As observed in the evolution of order parameters in (a) and (b), the rescaled Kuramoto network and the order-2 Kuramoto network exhibit equivalent stability of synchronization.

can be obtained for simulations that consider initial conditions far from the synchronization manifold. To describe the synchronization evolution over time, we utilize the global order parameter r. According to the mean-field theory in Ref.[54], we have $r(t)e^{i\Psi(t)} = 1/N\sum_{j=1}^{N} e^{i\theta(t)_j}$, where θ_j is the phase of the j-th node, Ψ is the averaged phase, r ranges from 0 to 1 , and $r = 1$ indicates the complete synchronization. If the perturbed system returns to $r = 1$ more quickly, it signifies greater stability of synchronization.

In Fig. 1(a), without rescaling, the order parameter of order-2 Kuramoto network (blue) hits the value 1 earlier than that of the order-1 Kuramoto network (yellow). This indicates that the perturbed system with higher-order interactions approaches the synchronous state faster than the order-1 Kuramoto network. However, upon introducing a rescaling to the order-1 Kuramoto network, the rescaled order-1 Kuramoto network (red) and the order-2 Kuramoto network (blue) achieve complete synchronized almost simultaneously. This outcome is a consequence of the rescaled Kuramoto network possessing the same synchronous stability as the higher-order ones. The same consequence can be observed in the case of the simplicial complex, as shown in Fig. 1(b). Figures. 1(c)-1(e) depict the phase evolution of individual nodes. The curves representing the order-1 Kuramoto network (yellow) are wider compared to those of the order-2 Kuramoto network (green). However, after rescaling, the curves of the rescaled order-1 Kuramoto network (red) closely resemble those of its higher-order counterparts, which indicates that the rescaled Kuramoto network and the higher-order Kuramoto network recover synchronization at a similar speed.

C. The rescaled multi-order Kuramoto network

In this section, we investigate a multi-order Kuramoto network that includes two interaction orders. Based on the analysis in Sec. II. B, we know that the coupled order-1 interactions $\sigma_1 \sum_{j_1=1}^{N} a_{ij_1}^{(1)} \sin(\theta_{j_1} - \theta_i)$ and the order-2 interactions $\sigma_2 \sum_{j_1=1}^{N}\sum_{j_2=1}^{N} a_{ij_1j_2}^{(2)} \sin(\theta_{j_1} + \theta_{j_2} - 2\theta_i)/R$ with rescaling contribute equally to the synchronization stability of a Kuramoto network. By combining these two orders, we construct a rescaled multi-order-2 Kuramoto network, given by

$$\begin{aligned}\dot{\theta}_i = \omega &+ \sigma_1 \sum_{j_1=1}^{N} a_{ij_1}^{(1)} \sin(\theta_{j_1} - \theta_i) \\ &+ \frac{\sigma_2}{R} \sum_{j_1=1}^{N}\sum_{j_2=1}^{N} a_{ij_1j_2}^{(2)} \sin(\theta_{j_1} + \theta_{j_2} - 2\theta_i).\end{aligned} \tag{10}$$

Following Refs.[45,49], in order to study the influence of higher-order interaction, a parameter α is introduced to adjust the proportion of higher order. To be consistent with Ref.[45], we set the coupling strength as $\sigma_1 = 1/ < k^{(1)} >, \sigma_2 = 1/\left(2 < k^{(2)} >\right)$, where $< k^{(d)} >$ is the average degree of order-d (see Appendix B for its definition). Consequently, the multi-order-2 Kuramoto network can be expressed as the following equation

$$\begin{aligned}\dot{\theta}_i = \omega &+ \frac{(1-\alpha)}{< k^{(1)} >} \sum_{j_1=1}^{N} a_{ij_1}^{(1)} \sin(\theta_{j_1} - \theta_i) \\ &+ \frac{\alpha}{2 < k^{(2)} >} \frac{1}{R} \sum_{j_1=1}^{N}\sum_{j_2=1}^{N} a_{ij_1j_2}^{(2)} \sin(\theta_{j_1} + \theta_{j_2} - 2\theta_i),\end{aligned} \tag{11}$$

where R is the rescaling defined in Eq. (8), which is

$$R = \frac{2\sigma_2 \boldsymbol{\lambda}_2\left(L^{(2)}\right)}{\sigma_1 \boldsymbol{\lambda}_2\left(L^{(1)}\right)} = \frac{< k^{(1)} > \boldsymbol{\lambda}_2\left(L^{(2)}\right)}{< k^{(2)} > \boldsymbol{\lambda}_2\left(L^{(1)}\right)}, \tag{12}$$

where $\boldsymbol{\lambda}_2\left(L^{(1)}\right)$ and $\boldsymbol{\lambda}_2\left(L^{(2)}\right)$ are the second eigenvalues of the generalized Laplacian $L^{(1)}$ and $L^{(2)}$.

Following Refs.[40,45], we investigate the synchronization stability of the rescaled multi-order Kuramoto network in Eq. (11) using the Maximum Transverse Lyapunov Exponent (MTLE), which refers to the maximum non-zero Lyapunov Exponent. The MTLE of Eq. (11) can be computed as the negative of the smallest non-zero eigenvalue of the multi-order Laplacian, which is described by

$$\Lambda_{\max}(\alpha) = -\boldsymbol{\lambda}_2\left(\frac{(1-\alpha)}{< k^{(1)} >} L^{(1)} + \frac{\alpha}{R < k^{(2)} >} L^{(2)}\right), \tag{13}$$

where $\boldsymbol{\lambda}_2 : \mathbb{R}^{(N\times N)} \to \mathbb{R}$ is a function that indicates the second eigenvalue of a matrix.

To compare the fixed normalization used in Refs.[40,45] with our rescaling, we calculate the MTLE in Eq. (13) of the rescaled multi-order-2 Kuramoto network in Eq. (11). In Figs. 2(a)-2(c), we consider a hypergraph with $p_1 = 0.1, p_2 = 0.02$

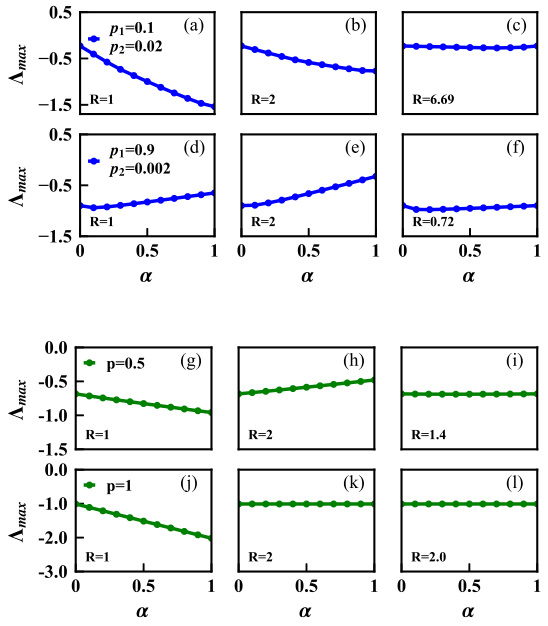

FIG. 2. (a)-(l) depict how the MTLEs change with the higher-order proportion α. (a)-(c) use the same hypergraph, whose the 1-hyperedge probability $p_1 = 0.1$ and 2-hyperedge probability $p_2 = 0.02$. For (a), the R in Eq. (10) is set to be 1. For (b), $R = 2$. For (c), $R = 6.69$, which is the rescaling calculated by Eq. (8). (d)-(f) are about another hypergraph, whose $p_1 = 0.9$ and $p_2 = 0.002$. Similarly, (g)-(i) display the MTLEs in a simplicial complex with the edge probability $p = 0.5$ and $R = 1$, $R = 2$, $R = 1.4$, respectively. (j)-(l) are for a simplicial complex with $p = 1$.

and evaluate its MTLE with R equal to 1, 2, and the rescaling factor 6.69 obtained from Eq. (12). Figs. 2(a), 2(b) demonstrate that with R equal to 1 or 2, the stability of synchronization is improved as α increases. But Fig. 2(c) with our rescaling $R = 6.69$ indicates a minimal change in synchronization stability. In Figs. 2(d)-2(f), a new hypergraph is generated with $p_1 = 0.9, p_2 = 0.002$. The MTLEs in Figs. 2(d), 2(e) adopt the same normalization factors as Figs. 2(a), 2(b), however, exhibiting different trends as compared to Figs. 2(a), 2(b). This comparison suggests that when using the same fixed normalization but different structures, different conclusions regarding the influence of higher-order interactions are reached. Figures. 2(g)-2(i) present the MTLEs of the rescaled multi-order-2 Kuramoto network in a simplicial complex with $p = 0.5$. Comparing Figs. 2(g) and 2(h), it is evident that for the same higher-order networks but different normalization factors, the MTLEs exhibit distinct behaviors. In Fig. 2(g), $R = 1$, the MTLE becomes smaller as α increases, indicating that higher-order interactions promote synchronization. However, in Fig. 2(h), $R = 2$, the MTLE follows an opposite trend. This discrepancy explains why Ref.[40] using $R = 1$ and Ref.[45] using $R = 2$ arrived at different conclusions regarding whether higher-order interactions in simplicial complexes promote synchronization stability. These comparisons demonstrate that the stability of networks with higher-order interactions is influenced not only by the representations of higher-order networks but also by specific network structures. Simply normalizing the coupling strength by the average degree and a fixed value of R for all higher-order structures may not be sufficient.

Note that in Figs. 2(k) and 2(l), $p = 1$ indicates an all-to-all connection between nodes. In this case, we can analytically calculate the rescaling, which is equal to 2 (see more details in Appendix B). This is the same as the normalization factor used in Ref.[45]. It indicates that the additional factor of 2 ensuring each interaction has an equal coupling weight regardless of the interaction order, is suitable for all-to-all connections. But for other connection structures, it may create bias towards specific orders. Therefore, to study the impact of higher-order interactions more fairly, it is essential to find a new rescaling factor.

In fact, the impact of higher-order interactions on synchronization is also related to the topology structures and coupling functions[39]. However, the normalization based on average degrees and interaction orders ignores the overall topology structures and coupling functions, which may not properly balance interactions of different orders. The rescaling defined in Eq. (5) considering coupling strength, topology structures, and coupling functions, aims to ensure that every order in a multi-order network contributes equally to the dynamics from the perspective of synchronization stability. It should be noted that the necessity of ensuring the same synchronization stability for each individual network in a multi-order network is reflected in the fact that if the higher-order network itself has stronger synchronization ability than the lower-order network, increasing the proportion of the higher-order term can easily lead to the conclusion that higher-order interactions promote synchronization.

Figures. 2(c), 2(f), 2(i), and 2(l) show that the values of rescaling vary with the network structures. When we rescale the order- 2 interactions using the structure dependent rescaling R, the stability of synchronization in the rescaled multi-order-2 Kuramoto network does not significantly change with α in both hypergraphs and simplicial complexes.

D. The stability of synchronization in the rescaled multi-order Kuramoto network

Now, to analyze the stability of synchronization in the rescaled multi-order- 2 Kuramoto network in a more detailed way, we address how its MTLE in Eq. (13) changes with α. We prove that this MTLE is a convex function, which means there is either an optimal α^* for the synchronization stability or the synchronization stability does not change with α.

Let $0 = \lambda_1 < \lambda_2 \leq \ldots \leq \lambda_N$ be eigenvalues of the generalized multi-order Laplacian $L^{(high)}$. The sum of its k smallest eigenvalues[55] is

$$\sum_{i=1}^{k} \lambda_i = \inf \left\{ \mathrm{Tr}\left(V^T L^{(high)} V \right) \mid V \in \mathbb{R}^{N\times k}, V^T V = 1 \right\}. \quad (14)$$

As the matrix multiplication and the trace of the matrix are

linear, thereby $\mathrm{Tr}\left(V^T L^{(high)} V\right)$ is a linear function. Then taking pointwise infimum over these linear (linear means both concave and convex) functions implies that $\sum_{i=1}^{k}\lambda_i$ is a concave function. As in Kuramoto networks, the MTLE $\Lambda_{\max}$ is equal to minus the second smallest eigenvalue of the Laplacian and $\lambda_1 = 0$, so that

$$\Lambda_{\max} = -\lambda_2 = -\sum_{i=1}^{2}\lambda_i \tag{15}$$

is a convex function. According to the properties of convex functions, the MTLE in Eq. (13) satisfies

$$\begin{aligned}\Lambda_{\max}(\alpha) &= -\boldsymbol{\lambda}_2\left(\frac{(1-\alpha)}{<k^{(1)}>}L^{(1)} + \frac{\alpha}{R<k^{(2)}>}L^{(2)}\right)\\ &\leq -(1-\alpha)\boldsymbol{\lambda}_2\left(\frac{L^{(1)}}{<k^{(1)}>}\right) - \alpha\boldsymbol{\lambda}_2\left(\frac{L^{(2)}}{R<k^{(2)}>}\right),\end{aligned} \tag{16}$$

that is the minus second eigenvalue of the sum of the normalized Laplacian (ESL), which is less than or equal to the minus sum of the second eigenvalue of the normalized Laplacian (SEL). By plugging $R = \left(<k^{(1)}>\boldsymbol{\lambda}_2\left(L^{(2)}\right)\right)/\left(<k^{(2)}>\boldsymbol{\lambda}_2\left(L^{(1)}\right)\right)$ defined in Eq. (12) into Eq. (16) (see more details in Appendix D), we obtain

$$\Lambda_{\max}(\alpha) \leq -\boldsymbol{\lambda}_2\left(\frac{L^{(1)}}{<k^{(1)}>}\right) = -\boldsymbol{\lambda}_2\left(\frac{L^{(2)}}{R<k^{(2)}>}\right), \tag{17}$$

that is $\Lambda_{\max}(\alpha) \leq \Lambda_{\max}(0) = \Lambda_{\max}(1), 0 < \alpha < 1$, which means the networks with only order-1 interactions $(\alpha = 0)$ or with the rescaled only order-2 interactions $(\alpha = 1)$ will have equivalent stability of synchronization $(\Lambda_{\max}(0) = \Lambda_{\max}(1))$. Besides, the upper bound of the MTLE, i.e., the right side of Eq. (16), is a constant function with α, which is equal to $\Lambda_{\max}(0)$ and $\Lambda_{\max}(1)$.

According to Eq. (16) and Eq. (17), the distance between the MTLE and its constant upper bound is

$$D(\alpha) = |\Lambda_{\max}(\alpha) - \Lambda_{\max}(0)|. \tag{18}$$

For example, in Fig. 3(a), the distance $d(\alpha)$ is equal to the absolute difference between the MTLE (blue dot line) and the constant upper bound (red dash line). The smaller the distance, the closer the MTLE is to a straight line.

Figures. 3(a), 3(d), 3(g) correspond to three cases of the MTLE, which are $\Lambda_{\max}(\alpha) < \Lambda_{\max}(0), \Lambda_{\max}(\alpha) \approx \Lambda_{\max}(0), \Lambda_{\max}(\alpha) = \Lambda_{\max}(0), 0 < \alpha < 1$. Next, we discuss the network structures and their stability of synchronization in each of these cases.

The top panel of Fig. 3 illustrates the hypergraphs with the same hyperedge probability but a varying number of nodes. For small hypergraphs, such as Fig. 3(a), the MTLE (blue) satisfies $\Lambda_{\max}(\alpha) < \Lambda_{\max}(0), 0 < \alpha < 1$. This indicates the existence of an optimal α^*, at which the MTLE $\Lambda_{\max}$ reaches its minimum, representing the most stable synchronization. Since $0 < \alpha^* < 1$ the optimal stable configuration does not consist solely of either lower-order interactions $(\alpha = 0)$ or with only higher-order interactions $(\alpha = 1)$. Therefore, it is not that higher order improves synchronization, but simply that these two topologies work together complementarily to provide the optimal stable configuration.

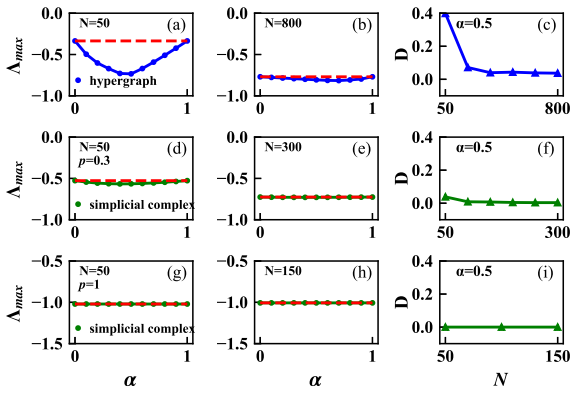

FIG. 3. (a)-(c) are about hypergraphs (blue) with the same hyperedge probability $p_1 = 0.2$ and $p_2 = 0.005$. The dot lines in (a), (b) illustrate the MTLEs of hypergraphs with the number of nodes $N = 50$ and $N = 800$, respectively. The red dash lines are their upper bound, which is a constant function with α. (c) shows that the distance between the MTLEs and their constant upper bound decays with the number of nodes N. (d)-(f) depict the MTLEs in Eq. (13) and the distance in Eq. (18) for simplicial complexes (green) with the edge probability $p = 0.3$. (g)-(i) depict the MTLEs and the distance for simplicial complexes with the edge probability $p = 1$. As shown in (g)-(i), in the all-to-all connected simplicial complex, the MTLE is a constant and the distance between the MTLEs and their upper bound is 0.

Then we increase the number of nodes, in Fig. 3(b), the MTLE (blue) is approximately equal to its constant upper bound (red), i.e., $\Lambda_{\max}(\alpha) \approx \Lambda_{\max}(0), 0 < \alpha < 1$. This is clearly shown in Fig. 3(c), where the distance decays with the number of nodes. This indicates that the MTLE is approaching a straight line, suggesting that having less or more higher order becomes irrelevant in very large networks.

The middle panel of Fig. 3 is about simplicial complexes with an edge probability $p = 0.3$. Even in a small network with $N = 50$, the MTLE is very close to its upper bound, implying that after rescaling, different order interactions have a similar influence on the stability of synchronization. This can be attributed to the characteristics of simplicial complexes. Unlike hyperedges, the higher-order simplexes in this study are formed by lower-order simplexes, which do not introduce new connections to the network. This implies that in the simplicial complex, the lower-order Laplacian and the higher-order Laplacian have the same zero elements and the underlying topology of simplicial complexes remains the same when adding the higher-order structure to it, which means the structures with different orders are similar, the change of the higher-order proportion α will not have a significant impact on the stability of synchronization.

The bottom panel of Fig. 3 focuses on simplicial complexes

with an edge probability $p = 1$, which means the connection in this simplicial complex is all-to-all. Fig. 3(i) shows that the distance defined in Eq. (18) is 0, indicating that for the all-to-all connection, we have $\Lambda_{\max}(\alpha) = \Lambda_{\max}(0)$, $0 < \alpha < 1$. In fact, we can prove that when the Laplacian $L^{(1)}$ and $L^{(2)}$ commute[56], the MTLE in Eq. (13) becomes a constant equal to its upper bound. As special cases, in simplicial complexes that encode all-to-all connection or m-nearest neighbors connection, the Laplacian matrices of any order commute (see more details in Appendix E). Therefore, through proper rescaling, the MTLE of these two types of higher-order networks does not change with α. Consequently, higher-order interactions in the all-to-all network and m-nearest neighbors network cannot promote or prevent the stability of synchronization.

By comparing the results in hypergraphs and simplicial complexes, such as Figs. 3(a) and 3(d). we articulate that when higher-order structures introduce new connections (as in hypergraphs), the optimal stable configuration includes both higher-order and lower-order interactions. This ensures that as more nodes are involved, the structure becomes better connected and more stable. On the other hand, if we only add higher-order interactions based on the existing connections (as in simplicial complexes), the connections are not expanded by higher-order structures, resulting in no significant impact on the stability of synchronization. Through the former analysis, we conclude that in the multi-order networks, the bigger the higher-order proportion does not mean the higher or lower synchronization stability. But rather there is an optimal proportion, which is highly dependent on the structure of the whole network.

III. DISCUSSION

There is nowadays strong mathematical support to determine the network configurations that lead to stable complete synchronous behavior. It is however still elusive whether natural systems being modeled by higher-order structures have evolved to that topology to promote or not synchronous behavior. This question is also pervasive to understand whether it is at all an advantage to construct networked systems with higher-order topology when the goal is to promote or prevent synchronization. This motivates this work, which seeks to understand rigorously the equivalence of the stability of the complete synchronous behavior for complex networks with different higher-order structures.

In this work, we have investigated the synchronization stability of a class of higher-order networks, characterized by constant or identical Jacobians of coupling functions across all orders. Our findings demonstrate that the synchronization stability of systems with different interaction orders can be made equivalent through appropriate rescaling. Further, by this rescaling, we introduce a method to build a rescaled multi-order network, in which each order of interactions contributes equally to synchronization stability. Our results show that in this rescaled network, compared to the pairwise interactions, higher-order interactions do not possess a unique impact on the stability of synchronization. Instead, it is the lower-order and higher-order topologies working together complementarily that provide the optimal stable configuration.

These results highlight the importance of considering network topology, coupling functions, and a proper rescaling factor in comprehending the role of higher-order interactions in synchronization stability. And the role of higher-order interactions could not be revealed without the constant rescaling proposed in this work.

SUPPLEMENTARY MATERIAL

In the supplementary material, we define the rescaling between an order-d network and a multi-order network, give examples of the Laplacian of a hypergraph and a simplicial complex, and provide other supplementary information.

AUTHOR CONTIBUTIONS

X.R. and M.S.B conceived the study and developed the theoretical framework. Y.L., C.G and M.S.B supervised the research and provided advice on the analysis. M.S.B and C.G. contributed to the results discussion. Y.L. contributed to the mathematical description of the multi-order network. X.R. carried out the simulations. All authors contributed to writing the manuscript.

DECLARATION OF COMPETING INTEREST

The authors declare no competing interests.

DATA AVAILABILITY STATEMENT

The data that support the findings of this study are available within the article.

ACKNOWLEDGMENTS

This work is supported by the National Natural Science Foundation of China (Grant No. 12072262).

IV. APPENDIXES

A. Hypergraphs and simplicial complexes

Hypergraphs and simplicial complexes are commonly used representations of higher-order interactions.

Hypergraphs[14]: A hypergraph $G = (V, E)$ is a generalization of the classical graph, in which V is the set of nodes and

E is the set of hyperedges. In a hypergraph, interactions between nodes are represented as hyperedges, which can connect any number of nodes. This property makes hypergraphs suitable for capturing many-body interactions.

Simplicial Complexes[57] : An M-dimensional simplicial complex S is a collection of simplices $S = \{\alpha_1, \alpha_2, \ldots, \alpha_M\}$ in which a d-dimensional simplex α_i is formed by connecting a set of nodes, $\alpha_i = [v_0, v_1, \ldots, v_d]$. For example, a 1 -simplex $[v_0, v_1]$ is an edge that connects two nodes, and a 2-simplex $[v_0, v_1, v_2]$ is a triangle that connects three nodes. A simplicial complex is a type of hypergraph with an extra condition that if a simplex exists, then all of its subsets must also exist. For example, if a triangle $[v_0, v_1, v_2]$ exists, then the edges and vertices that make up the triangle must also exist, i.e., $S = \{[v_0, v_1, v_2], [v_0, v_1], [v_0, v_2], [v_1, v_2], [v_0], [v_1], [v_2]\}$.

We consider these two topologies to generate our Kuramoto networks. The method described in Ref.[45] is followed for generating the random hypergraphs and simplicial complexes. In the randomly generated hypergraphs[58], each hyperedge with dimension d is formed by selecting any $d+1$ from the total N nodes with edge probabilities p_d. Hyperedges containing different numbers of nodes are independent. So that additional connections among nodes can be established by introducing higher-order hyperedges. In the case of simplicial complexes, the generation process involves the following steps. First, 1-simplexes are generated from an Erdös-Rényi graph[59] with edge probability p. Then, 2-simplexes are recognized from interconnected 1-simplexes. Specifically, if the 1-simplexes $(i, j), (j, k), (i, k)$ exist, then a 2 -simplex (i, j, k) is formed.

According to the way we generate the simplicial complexes, the presence of lower-order interactions determines the existence of higher-order interactions. That is, higher-order simplexes only add higher-order interactions without adding new connections. The underlying network topology of the higher-order structure and the lower-order structure remains the same.

B. The generalized higher-order Laplacian

The Laplacian matrix is a useful tool for analyzing the dynamics and stability of coupled units. Recently, the Laplacian matrix was generalized to incorporate higher-order interactions. Following the definition in Ref.[39], the generalized Laplacian of order d is

$$L_{ij}^{(d)} = d!k_i^{(d)}\delta_{ij} - (d-1)!k_{ij}^{(d)}, \tag{B1}$$

$$k_i^{(d)} = \frac{1}{d!}\sum_{i_1=1}^{N}\sum_{i_2=1}^{N}\cdots\sum_{i_d=1}^{N} a_{i,i_1,i_2,\ldots,i_d}^{(d)}, \tag{B2}$$

$$k_{ij}^{(d)} = \frac{1}{(d-1)!}\sum_{i_1=1}^{N}\sum_{i_2=1}^{N}\cdots\sum_{i_{d-1}=1}^{N} a_{i,j,i_1,i_2,\ldots,i_{d-1}}^{(d)}, \tag{B3}$$

where δ_{ij} is the Kronecker delta, i.e., $\delta_{ij} = 1$ if $i = j$, else $\delta_{ij} = 0$. The generalized d-degree $k_i^{(d)}$ indicates the number of distinct d-simplices incident to each node. The order-d adjacency matrix $\left(k_{ij}^{(d)}\right)$ represents the number of distinct d-simplices incident to each pair of nodes (i, j).

Note that this definition is a bit different from that in the Ref.[39]. Because we study the higher-order networks both represented by simplicial complexes and hypergraphs. If the network is a hypergraph, when $a_{ij}^{(1)} = 0, L_{ij}^{(d)}$ does not have to be zero, but if it is a simplicial complex, $L_{ij}^{(d)}$ must be zero. What's more, as we recognize the interconnected lower-order simplexes as a higher-order simplex, the Laplacian of all orders have the same zero elements.

When the connection is all-to-all, we can express $L^{(d)}$ of any order with $L^{(1)}$. For order 1, $k_i^{(1)} = N-1, k_{ij}^{(1)} = (1-\delta_{ij})$. According to the analysis in the Ref.[40],

$$k_i^{(d)} = \binom{N-1}{d} = \frac{(N-2)\ldots(N-d)}{d!}k_i^{(1)}, \tag{B4}$$

$$k_{ij}^{(d)} = \binom{N-2}{d-1}(1-\delta_{ij}) == \frac{(N-2)\ldots(N-d)}{(d-1)!}k_{ij}^{(1)}. \tag{B5}$$

Then the generalized Laplacian of order d is

$$\begin{aligned} L_{ij}^{(d)} &= d!k_i^{(d)}\delta_{ij} - (d-1)!k_{ij}^{(d)} \\ &= (N-2)\ldots(N-d)\left(k_i^{(1)}\delta_{ij} - k_{ij}^{(1)}\right). \\ &= (N-2)\ldots(N-d)L_{ij}^{(1)} \end{aligned} \tag{B6}$$

As $\lambda_2\left(L^{(1)}\right) = N$ the second eigenvalue of $L^{(d)}$ is $\lambda_2\left(L^{(d)}\right) = N(N-2)\ldots(N-d)$. By plugging the average degrees $< k^{(1)} >= N-1, \left\langle k^{(2)}\right\rangle = (N-1)(N-2)/2$, the second eigenvalues $\lambda_2\left(L^{(1)}\right) = N, \lambda_2\left(L^{(2)}\right) = N(N-2)$ into Eq. (12), we get that the rescaling is equal to 2.

C. The Jacobian of coupling function in the Kuramoto model

The order-d coupling function of the Kuramoto model is $g^{(d)}\left(\theta_i, \theta_{j_1}, \ldots, \theta_{j_d}\right) = \sin\left(\sum_{k=1}^{d}\theta_{j_k} - d\theta_i\right)$. Its Jacobian is described as $JG^{(d)} = \sum_{k=1}^{d} J_k g^{(d)}$, where

$$\begin{aligned} J_k g^{(d)} &= \left.\frac{\partial \sin\left(\sum_{k=1}^{d}\theta_{j_k} - d\theta_i\right)}{\partial\theta_{j_k}}\right|_{(\theta^s,\ldots,\theta^s)} \\ &= \left.\cos\left(\sum_{k=1}^{d}\theta_{j_k} - d\theta_i\right)\right|_{(\theta^s,\ldots,\theta^s)} \\ &= \cos(0) = 1, k = 1, 2, \ldots, d. \end{aligned} \tag{C1}$$

So that $JG^{(d)} = \sum_{k=1}^{d} J_k g^{(d)} = d$, which means in the Kuramoto model the Jacobian of its coupling function at the synchronous solution $\theta^s = \theta_1 = \theta_2 = \ldots = \theta_N$ is constant.

D. The constant upper bound of the MTLE

By plugging $R = \left(< k^{(1)} > \boldsymbol{\lambda}_2\left(L^{(2)}\right)\right) / \left(< k^{(2)} > \boldsymbol{\lambda}_2\left(L^{(1)}\right)\right)$ into $\boldsymbol{\lambda}_2\left(L^{(2)}/R < k^{(2)} >\right)$, we get

$$\boldsymbol{\lambda}_2\left(\frac{L^{(2)}}{R < k^{(2)} >}\right) = \boldsymbol{\lambda}_2\left(\frac{\boldsymbol{\lambda}_2\left(L^{(1)}\right)L^{(2)}}{< k^{(1)} > \boldsymbol{\lambda}_2\left(L^{(2)}\right)}\right) = \boldsymbol{\lambda}_2\left(\frac{L^{(1)}}{< k^{(1)} >}\right). \tag{D1}$$

Then Eq. (16) becomes

$$\begin{aligned}
\Lambda_{\max}(\alpha) &\leq -(1-\alpha)\boldsymbol{\lambda}_2\left(\frac{L^{(1)}}{< k^{(1)} >}\right) - \alpha\boldsymbol{\lambda}_2\left(\frac{L^{(2)}}{R < k^{(2)} >}\right) \\
&= -(1-\alpha)\boldsymbol{\lambda}_2\left(\frac{L^{(1)}}{< k^{(1)} >}\right) - \alpha\boldsymbol{\lambda}_2\left(\frac{\boldsymbol{\lambda}_2\left(L^{(1)}\right)L^{(2)}}{< k^{(1)} > \boldsymbol{\lambda}_2\left(L^{(2)}\right)}\right) \\
&= -\boldsymbol{\lambda}_2\left(\frac{L^{(1)}}{< k^{(1)} >}\right) + \alpha\boldsymbol{\lambda}_2\left(\frac{L^{(1)}}{< k^{(1)} >}\right) - \alpha\boldsymbol{\lambda}_2\left(\frac{L^{(1)}}{< k^{(1)} >}\right) \\
&= -\boldsymbol{\lambda}_2\left(\frac{L^{(1)}}{< k^{(1)} >}\right) = \boldsymbol{\lambda}_2\left(\frac{L^{(2)}}{R < k^{(2)} >}\right).
\end{aligned} \tag{D2}$$

From Eq. (D2), we know that $\Lambda_{\max}(0) = \Lambda_{\max}(1)$ and $\Lambda_{\max}(\alpha) \leq \Lambda_{\max}(0) = \Lambda_{\max}(1), 0 < \alpha < 1$. The upper bound of the MTLE is determined by $L^{(1)}$ and $\left\langle k^{(1)} \right\rangle$, which is a constant function with α.

E. When the MTLE is equal to its upper bound

According to Eq. (16) and Eq. (17), $\Lambda_{\max}(\alpha) = \Lambda_{\max}(0) = \Lambda_{\max}(1)$ can be expanded as

$$\begin{aligned}
\Lambda_{\max}(\alpha) &= -\boldsymbol{\lambda}_2\left(\frac{(1-\alpha)}{< k^{(1)} >}L^{(1)} + \frac{\alpha}{R < k^{(2)} >}L^{(2)}\right) \\
&= -(1-\alpha)\boldsymbol{\lambda}_2\left(\frac{L^{(1)}}{< k^{(1)} >}\right) - \alpha\boldsymbol{\lambda}_2\left(\frac{L^{(2)}}{R < k^{(2)} >}\right) \\
&= -\boldsymbol{\lambda}_2\left(\frac{L^{(1)}}{< k^{(1)} >}\right) = -\boldsymbol{\lambda}_2\left(\frac{L^{(2)}}{R < k^{(2)} >}\right).
\end{aligned} \tag{E1}$$

As a special case, if the Laplacian $L^{(1)}$ and $L^{(2)}$ commute, Eq. (E1) holds. Because the commuting matrices can be simultaneously diagonalized by the same invertible matrix, this implies the existence of a matrix P satisfying

$$\begin{aligned}
&P^{-1}\left(\frac{(1-\alpha)}{< k^{(1)} >}L^{(1)} + \frac{\alpha}{R < k^{(2)} >}L^{(2)}\right)P \\
&= \frac{(1-\alpha)}{< k^{(1)} >}P^{-1}L^{(1)}P + \frac{\alpha}{R < k^{(2)} >}P^{-1}L^{(2)}P = \mathrm{diag}\left(\lambda_1, \ldots, \lambda_N\right).
\end{aligned} \tag{E2}$$

Based on this, we obtain that the eigenvalues of the sum of Laplacian matrices are equal to the sum of the eigenvalues of the Laplacian matrices (i.e., $\boldsymbol{\lambda}_i\left(L^{(1)} + L^{(2)}\right) = \boldsymbol{\lambda}_i\left(L^{(1)}\right) + \boldsymbol{\lambda}_i\left(L^{(2)}\right), i = 1, 2, \ldots, N$). As the MTLE is the negative of the second eigenvalue of the Laplacian matrix, Eq. (E1) is proven.

In the case where the topology of the simplicial complex corresponds to either an all-to-all connection or an m-nearest neighbors connection, the Laplacian matrices $L^{(1)}$ and $L^{(2)}$ can be shown to be circulant matrices. And circulant matrices commute[60]. Therefore, for these two topologies, $L^{(1)}$ and $L^{(2)}$ commute, then Eq. (E1) holds. Consequently, the MTLE is equal to its upper bound, which is a constant function with α.

[1] S. Boccaletti, V. Latora, Y. Moreno, M. Chavez, and D.-U. Hwang, "Complex networks: Structure and dynamics," Physics reports **424**, 175–308 (2006).

[2] A. Barrat, M. Barthelemy, and A. Vespignani, *Dynamical processes on complex networks* (Cambridge university press, 2008).

[3] G. A. Pavlopoulos, M. Secrier, C. N. Moschopoulos, T. G. Soldatos, S. Kossida, J. Aerts, R. Schneider, and P. G. Bagos, "Using graph theory to analyze biological networks," BioData mining **4**, 1–27 (2011).

[4] G. Petri, P. Expert, F. Turkheimer, R. Carhart-Harris, D. Nutt, P. J. Hellyer, and F. Vaccarino, "Homological scaffolds of brain functional networks," Journal of The Royal Society Interface **11**, 20140873 (2014).

[5] A. E. Sizemore, C. Giusti, A. Kahn, J. M. Vettel, R. F. Betzel, and D. S. Bassett, "Cliques and cavities in the human connectome," Journal of computational neuroscience **44**, 115–145 (2018).

[6] J. Grilli, G. Barabás, M. J. Michalska-Smith, and S. Allesina, "Higher-order interactions stabilize dynamics in competitive network models," Nature **548**, 210–213 (2017).

[7] P. Singh and G. Baruah, "Higher order interactions and species coexistence," Theoretical Ecology **14**, 71–83 (2021).

[8] A. Patania, G. Petri, and F. Vaccarino, "The shape of collaborations. epj data sci 6 (18)," (2017).

[9] E. Vasilyeva, A. Kozlov, K. Alfaro-Bittner, D. Musatov, A. Raigorodskii, M. Perc, and S. Boccaletti, "Multilayer representation of collaboration networks with higher-order interactions," Scientific reports **11**, 5666 (2021).

[10] F. Battiston, E. Amico, A. Barrat, G. Bianconi, G. Ferraz de Arruda, B. Franceschiello, I. Iacopini, S. Kéfi, V. Latora, Y. Moreno, *et al.*, "The physics of higher-order interactions in complex systems," Nature Physics **17**, 1093–1098 (2021).

[11] S. Boccaletti, P. De Lellis, C. del Genio, K. Alfaro-Bittner, R. Criado, S. Jalan, and M. Romance, "The structure and dynamics of networks with higher order interactions," Physics Reports **1018**, 1–64 (2023).

[12] T. Carletti, D. Fanelli, and S. Nicoletti, "Dynamical systems on hypergraphs," Journal of Physics: Complexity **1**, 035006 (2020).

[13] G. Ferraz de Arruda, M. Tizzani, and Y. Moreno, "Phase transitions and stability of dynamical processes on hypergraphs," Communications Physics **4**, 24 (2021).

[14] S. Adhikari, J. G. Restrepo, and P. S. Skardal, "Synchronization of phase oscillators on complex hypergraphs," Chaos: An Interdisciplinary Journal of Nonlinear Science **33** (2023).

[15] I. Iacopini, G. Petri, A. Barrat, and V. Latora, "Simplicial models of social contagion," Nature communications **10**, 2485 (2019).

[16] D. Zhao, R. Li, H. Peng, M. Zhong, and W. Wang, "Higher-order percolation in simplicial complexes," Chaos, Solitons & Fractals **155**, 111701 (2022).

[17] M. Barahona and L. M. Pecora, "Synchronization in small-world systems," Physical review letters **89**, 054101 (2002).

[18] A. Arenas, A. Díaz-Guilera, J. Kurths, Y. Moreno, and C. Zhou, "Synchronization in complex networks," Physics reports **469**, 93–153 (2008).

[19] J. Cao and J. Lu, "Adaptive synchronization of neural networks with or without time-varying delay," Chaos: An Interdisciplinary Journal of Nonlinear Science **16** (2006).

[20] M. Baptista, F. M. Kakmeni, and C. Grebogi, "Combined effect of chemical and electrical synapses in hindmarsh-rose neural networks on synchronization and the rate of information," Physical Review E **82**, 036203 (2010).

[21] R. R. Borges, F. S. Borges, E. L. Lameu, P. R. Protachevicz, K. C. Iarosz, I. L. Caldas, R. L. Viana, E. E. Macau, M. S. Baptista, C. Grebogi, *et al.*, "Synaptic plasticity and spike synchronisation in neuronal networks," Brazilian Journal of Physics **47**, 678–688 (2017).

[22] P. R. Protachevicz, F. da Silva Borges, A. M. Batista, M. da Silva Baptista, I. L. Caldas, E. E. N. Macau, and E. L. Lameu, "Plastic neural network with

transmission delays promotes equivalence between function and structure," Chaos, Solitons & Fractals **171**, 113480 (2023).
[23]B. M. Sadler and A. Swami, "Synchronization in sensor networks: an overview," in *MILCOM 2006-2006 IEEE Military Communications conference* (IEEE, 2006) pp. 1–6.
[24]W.-X. Wang, X. Ni, Y.-C. Lai, and C. Grebogi, "Pattern formation, synchronization, and outbreak of biodiversity in cyclically competing games," Physical Review E **83**, 011917 (2011).
[25]M. S. Baptista, R. M. Szmoski, R. F. Pereira, and S. d. S. Pinto, "Chaotic, informational and synchronous behaviour of multiplex networks," Scientific Reports **6**, 22617 (2016).
[26]F. Della Rossa, L. Pecora, K. Blaha, A. Shirin, I. Klickstein, and F. Sorrentino, "Symmetries and cluster synchronization in multilayer networks," Nature communications **11**, 3179 (2020).
[27]Y. Meng, Y.-C. Lai, and C. Grebogi, "The fundamental benefits of multiplexity in ecological networks," Journal of the Royal Society Interface **19**, 20220438 (2022).
[28]V. Kohar, P. Ji, A. Choudhary, S. Sinha, and J. Kurths, "Synchronization in time-varying networks," Physical Review E **90**, 022812 (2014).
[29]P. S. Skardal and A. Arenas, "Higher order interactions in complex networks of phase oscillators promote abrupt synchronization switching," Communications Physics **3**, 218 (2020).
[30]R. Ghorbanchian, J. G. Restrepo, J. J. Torres, and G. Bianconi, "Higher-order simplicial synchronization of coupled topological signals," Communications Physics **4**, 120 (2021).
[31]A. D. Kachhvah and S. Jalan, "First-order route to antiphase clustering in adaptive simplicial complexes," Physical Review E **105**, L062203 (2022).
[32]C. Xu, Y. Zhai, Y. Wu, Z. Zheng, and S. Guan, "Enhanced explosive synchronization in heterogeneous oscillator populations with higher-order interactions," Chaos, Solitons & Fractals **170**, 113343 (2023).
[33]T. Tanaka and T. Aoyagi, "Multistable attractors in a network of phase oscillators with three-body interactions," Physical Review Letters **106**, 224101 (2011).
[34]P. S. Skardal and A. Arenas, "Abrupt desynchronization and extensive multistability in globally coupled oscillator simplexes," Physical review letters **122**, 248301 (2019).
[35]S. Kundu and D. Ghosh, "Higher-order interactions promote chimera states," Physical Review E **105**, L042202 (2022).
[36]X. Li, D. Ghosh, and Y. Lei, "Chimera states in coupled pendulum with higher-order interaction," Chaos, Solitons & Fractals **170**, 113325 (2023).
[37]D. K. Umberger, C. Grebogi, E. Ott, and B. Afeyan, "Spatiotemporal dynamics in a dispersively coupled chain of nonlinear oscillators," Physical Review A **39**, 4835 (1989).
[38]F. Sorrentino, "Synchronization of hypernetworks of coupled dynamical systems," New Journal of Physics **14**, 033035 (2012).
[39]L. V. Gambuzza, F. Di Patti, L. Gallo, S. Lepri, M. Romance, R. Criado, M. Frasca, V. Latora, and S. Boccaletti, "Stability of synchronization in simplicial complexes," Nature communications **12**, 1255 (2021).
[40]M. Lucas, G. Cencetti, and F. Battiston, "Multiorder laplacian for synchronization in higher-order networks," Physical Review Research **2**, 033410 (2020).
[41]J. A. Acebrón, L. L. Bonilla, C. J. P. Vicente, F. Ritort, and R. Spigler, "The kuramoto model: A simple paradigm for synchronization phenomena," Reviews of modern physics **77**, 137 (2005).
[42]P. H. Nardelli, N. Rubido, C. Wang, M. S. Baptista, C. Pomalaza-Raez, P. Cardieri, and M. Latva-aho, "Models for the modern power grid," The European Physical Journal Special Topics **223**, 2423–2437 (2014).
[43]F. A. Rodrigues, T. K. D. Peron, P. Ji, and J. Kurths, "The kuramoto model in complex networks," Physics Reports **610**, 1–98 (2016).
[44]C. Wang, C. Grebogi, and M. S. Baptista, "One node driving synchronisation," Scientific Reports **5**, 18091 (2015).
[45]Y. Zhang, M. Lucas, and F. Battiston, "Higher-order interactions shape collective dynamics differently in hypergraphs and simplicial complexes," Nature Communications **14**, 1605 (2023).
[46]L. Gallo, R. Muolo, L. V. Gambuzza, V. Latora, M. Frasca, and T. Carletti, "Synchronization induced by directed higher-order interactions," Communications Physics **5**, 263 (2022).
[47]M. S. Anwar and D. Ghosh, "Stability of synchronization in simplicial complexes with multiple interaction layers," Physical Review E **106**, 034314 (2022).
[48]P. S. Skardal, L. Arola-Fernández, D. Taylor, and A. Arenas, "Higher-order interactions can better optimize network synchronization," Physical Review Research **3**, 043193 (2021).
[49]M. Manoranjani, D. Senthilkumar, and V. Chandrasekar, "Abrupt desynchronization and abrupt transition to π-state in globally coupled oscillator simplexes with contrarians and conformists," Chaos, Solitons & Fractals **167**, 113018 (2023).
[50]E. S. Medeiros, U. Feudel, and A. Zakharova, "Asymmetry-induced order in multilayer networks," Physical Review E **104**, 024302 (2021).
[51]Y. Tang, D. Shi, and L. L$^{\text{"}}$u, "Optimizing higher-order network topology for synchronization of coupled phase oscillators," Communications Physics **5**, 96 (2022).
[52]L. M. Pecora and T. L. Carroll, "Master stability functions for synchronized coupled systems," Physical review letters **80**, 2109 (1998).
[53]L. Huang, Q. Chen, Y.-C. Lai, and L. M. Pecora, "Generic behavior of master-stability functions in coupled nonlinear dynamical systems," Physical Review E **80**, 036204 (2009).
[54]H. Hong and S. H. Strogatz, "Kuramoto model of coupled oscillators with positive and negative coupling parameters: An example of conformist and contrarian oscillators," Physical Review Letters **106**, 054102 (2011).
[55]S. P. Boyd and L. Vandenberghe, *Convex optimization* (Cambridge university press, 2004).
[56]R. A. Horn and C. R. Johnson, *Matrix analysis* (Cambridge university press, 2012).
[57]G. Bianconi, *Higher-order networks* (Cambridge University Press, 2021).
[58]M. Dewar, J. Healy, X. Pérez-Giménez, P. Prałat, J. Proos, B. Reiniger, and K. Ternovsky, "Subhypergraphs in non-uniform random hypergraphs," arXiv preprint arXiv:1703.07686 (2017).
[59]L. Erdős, A. Knowles, H.-T. Yau, and J. Yin, "Spectral statistics of erdős-rényi graphs ii: Eigenvalue spacing and the extreme eigenvalues," Communications in Mathematical Physics **314**, 587–640 (2012).
[60]D. Shemesh, "Common eigenvectors of two matrices," Linear algebra and its applications **62**, 11–18 (1984).